Discrete elemental parameter calibration of the bonding model for caking compound fertilizer utilized in oilseed rape mechanized direct seeding

Wenli Xiao[1,2], Qingxi Liao[1,2*], Yitao Liao[1,2], Lei Wang[1,2], Xingyu Wan[1,2]

(1. *College of Engineering, Huazhong Agricultural University, Wuhan 430070, China*;
2. *Key Laboratory of Agricultural Equipment in Mid-lower Yangtze River, Ministry of Agriculture and Rural Affairs, Wuhan 430070, China*)

Abstract: To address the problem that granular compound fertilizer is prone to agglomeration during mechanized direct seeding of oilseed rape in the middle and lower reaches of the Yangtze River, which causes clogging of the fertilizer discharger and leads to a reduction in the uniformity and stability of fertilizer discharge, research on the crushing mechanism of caking compound fertilizer was performed. Considering that it is difficult to measure the bonding force between caking fertilizer particles directly, a simulation model of caking composite fertilizer was established with the bonding model in EDEM discrete element software. To decrease error between the simulation and physical test results, the normal contact stiffness, tangential contact stiffness, critical normal stress, critical tangential stress, bonding radius, and other parameters of the bonding model of caking composite fertilizer were calibrated. The three-dimensional structure of the caking composite fertilizer was obtained via three-dimensional scanning, the critical crushing displacement and critical crushing force of the caking composite fertilizer were measured via compression testing with a mass spectrometer, and the optimal parameter combination of the bonding model was determined via EDEM discrete element simulation of the Plackett-Burman test, steepest ascent test, and Box-Behnken test. The results of the simulated compression tests under the optimal parameter combination show that the relative errors of the critical crushing displacement and critical crushing force with respect to the physical test results were 0.296% and 0.343%, respectively. Using the crushing rate of caking compound fertilizer as an evaluation index, the feasibility of the calibrated parameters was verified for a four-head spiral two-row fertilizer discharger installed in a direct seeding machine for oilseed rape. The results show that the relative errors of the caking fertilizer crushing rates from the simulation relative to those of the bench and field tests were 5.81% and 5.06%, respectively, indicating that the calibration parameters of the discrete element model were accurate and could be used for parameter analysis of caking fertilizer with a discrete element model. These results can provide a reference for the structural optimization of fertilizer discharger crushing of caking fertilizer of direct seeding machine for oilseed rape.

Keywords: caking compound fertilizer, bonding model, three-dimensional scanning, parameter calibration, discrete element method

DOI: 10.25165/j.ijabe.20251804.9201

Citation: Xiao W L, Liao Q X, Liao Y T, Wang L, Wan X Y. Discrete elemental parameter calibration of the bonding model for caking compound fertilizer utilized in oilseed rape mechanized direct seeding. Int J Agric & Biol Eng, 2025; 18(4): 17–25.

1 Introduction

Oilseed rape is an important oil crop in China, and the national oilseed rape planting area is more than 7.33 million hm^2[1]. Overall, conditions for oilseed rape planting in China are poor, the soil fertility level is low, and fertilization plays a key role in guaranteeing stable yield and harvest of oilseed rape and quality enhancement[2,3]. With respect to rapeseed, mechanized direct seeding universal application, and agricultural production weight loss efficiency policy, how to improve the quality of oilseed rape direct seeding and fertilization has become a key issue facing the mechanized direct application of oilseed rape seeds and fertilizer[4,5]. Compound fertilizer agglomerates during long-term storage due to the influence of particle size, hygroscopicity, particle strength, and other factors[6,7]. The caking fertilizer will arch and block the fertilizer discharge port in the fertilizer tank, leading to fertilizer breakup during the mechanized direct seeding of oilseed rape and affecting the growth and development of direct-seeded oilseed rape[8]. The adaptability of the fertilizer discharge device to the fertilizer form affects the quality of fertilizer application, and the analysis of the interaction and crushing mechanism between the caking fertilizer and the fertilizer discharge device during the process of fertilizer discharge can provide a basis for improving the design of fertilizer discharge devices[9,10].

A bonding model is proposed based on the research of Potyondy and Cundall; this model is a contact model for discrete element simulation and is often used to simulate material breakage[11]. Small particles are bonded to form large particles through bonds, which have mechanical properties; breakage is mainly determined by five bonding parameters, namely, the normal contact stiffness, tangential contact stiffness, critical normal stress, critical tangential stress, and bonding radius[12,13]. When the external force or moment exceeds the bond force or the distance between small particles exceeds the set contact radius, the bond between particles breaks, and crushing occurs[14]. The bonding model is

Received date: 2024-07-04 **Accepted date:** 2025-03-18

Biographies: Wenli Xiao, Engineer, research interest: technology and equipment of mechanized production of oilseed rape, Email: xiaowl@mail.hzau.edu.cn; **Yitao Liao**, Professor, research interest: technology and equipment of mechanized production of oilseed rape, Email: liaoetao@mail.hzau.edu.cn; **Lei Wang**, PhD, research interest: technology and equipment of mechanized production of oilseed rape, Email: wangchong12356@126.com; **Xingyu Wan**, Associate professor, research interest: harvesting technology and equipment of oilseed rape, Email: wanxy@mail.hzau.edu.cn.

***Corresponding author: Qingxi Liao**, Professor, research interest: technology and equipment of mechanized production of oilseed rape. No.1 Shizishan Street, Hongshan District, Wuhan 430070, China. Email: liaoqx@mail.hzau.edu.cn.

widely used in the modeling of concrete and rock structures and has been widely used in the fields of rock mechanics, mining engineering, etc.[15]. There are more studies on straw crushing by the bonding model in the field of agriculture[16,17]. Liao et al.[18,19] used the maximum load of fodder rape stalk bending damage as a reference value and analyzed and determined the main simulation parameters of the discrete element bonding model for fodder rape stalk. Zhang et al.[20], using the CCD principle, analyzed the significance of the effect of the bonding parameter on the destructive load, optimally derived the bonding parameters of the bonding model obtained for cotton straw, and verified the feasibility of the parameters. Zhang et al.[21] calibrated the parameters of the bonding contact model of corn stover through uniaxial compression simulation and bench tests and verified it by crushing simulation and tests. They also calibrated the bonding parameters of a discrete element bonding model of banana straw by comparing physical and simulation shear test results and verified the reliability of the simulation results in terms of physical test results[22]. The above studies show that the discrete element simulation bonding model has been effectively applied in crop straw research.

Domestic scholars have carried out in-depth research on the application of the bonding model to organic fertilizer crushing[23,24]. Yuan et al.[25] used the maximum load and corresponding displacement of the uniaxial compression test as a reference, and based on the uniaxial compression simulation test, they searched for and obtained the optimal bonding parameter combinations of organic fertilizer blocks for the bonding model. Chen et al.[26] set up a crushing model of organic fertilizer blocks and set the bonding parameters of the bonding model by considering the relevant literature. Du et al.[27] took the film-coated fertilizer ultimate crushing displacement and ultimate crushing load simulation results targets to determine the optimal combination of bonding model parameters for coated fertilizer. They used the crushing rate as an indicator and an external grooved wheel fertilizer discharger to verify the reliability of the parameters. Currently, there are few studies on granular fertilizer caking and crushing. To ensure the authenticity of the simulation of caking fertilizer crushing and to provide reliable parameters for caking fertilizer simulation analysis, it is necessary to calibrate the simulation parameters of the caking compound fertilizer bonding model.

To address the problem of reduced uniformity and stability of fertilizer discharge due to fertilizer caking in the process of mechanized oilseed rape fertilizer application in the middle and lower reaches of the Yangtze River, the critical crushing displacement and critical crushing force of caking fertilizer were obtained by using compression tests of the apparatus, and a discrete metamodel with structural characteristics close to those of real caking fertilizer was established by three-dimensional scanning and particle replacement. Plackett–Burman, steepest ascent, and Box–Behnken tests were used to determine the parameters with the most significant influence and narrow the relevant ranges of the parameters, and optimization was used to obtain a better bonding model parameter combination to more closely simulate real crushing tests. To verify the accuracy of the parameter combinations, a four-head spiral two-row fertilizer discharger was used to simulate the crushing rate of caking fertilizers with bench and field discharge tests, and the crushing rates of caking fertilizers from the simulation and the bench and field tests were compared and analyzed to determine a suitable solution for improving the crushing rate of caking fertilizer. This study provides a reference for the optimization of the structure of mechanized direct seeding fertilizer dischargers for oilseed rape to adapt to the crushing of caking fertilizer.

2 Materials and methods

2.1 Structure of the direct seed machine and the process of fertilizer discharging

The precision direct seeding machine for oilseed rape is mainly composed of a rotary cutting and leveling device, seed discharging system, fertilizer discharging system, furrow opening device, and other components (Figure 1a). The fertilizer discharging system includes a fertilizer discharger, a fertilizer discharge pipe, and a deep loosening fertilizer application device. The main structure of the fertilizer discharger is shown in Figure 1b.

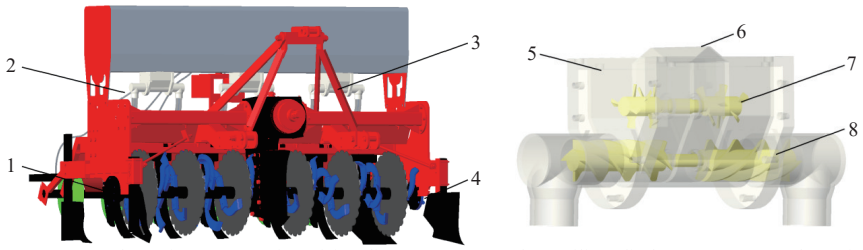

a. Schematic structure of precision direct seeding machine for oilseed rape

b. Fertilizer discharger structure schematic

1. Rotary cutting and leveling device 2. Seed discharging system 3. Fertilizer discharging system 4. Furrowing system 5. Fertilizer discharge housing 6. Fertilizer distributor 7. Knot breaker 8. Fertilizer discharge screw

Figure 1 Structure of precision planter for rapeseed and its key components

During operation, fertilizer moves from the fertilizer box through the fertilizer diverter into the two sides of the fertilizer discharging cavity, a broken knot device for fertilizer mixing and lump crushing, improving the uniformity of fertilizer falling and preventing a fertilizer arch due to moisture causing the nonuniform discharge of fertilizer. Then, the fertilizer is stirred by the discharger screws, which convey the fertilizer into the discharge pipe to achieve the desired fertilizer depth of the cultivation layer.

2.2 Bonding modeling of caking fertilizer

The bonding force between particles of caking fertilizer is difficult to determine, and the bonding model in EDEM (EDEM2020, Altair, USA) can be used to simulate the separation of particles of caking fertilizers by setting the parameters of interparticle bonding to simulate the process of caking fertilizer fragmentation to simulate and analyze the crushing process of caking fertilizer. The parameter setting in the model directly affects the credibility of the caking fertilizer crushing simulation, and the parameter calibration can improve the simulation accuracy.

The test fertilizer used was mother and daughter red compound fertilizer, as shown in Figure 2. The fertilizer capacity was

915.3 kg/m^3, the moisture content was 1.77%, the dimensions along three orthogonal axes were 4.12 mm, 3.79 mm, and 2.59 mm, and the equivalent diameter was 3.44 mm. After mechanized direct seeding of the oilseed rape in the fertilizer tank, for three-dimensional scanning, the standard caking fertilizer size was assumed to plug the adopted four-head spiral two-row fertilizer during discharge as a reference basis[5]. After scanning with caking fertilizer, the dimensions along the same three orthogonal axes were 45.2 mm, 35.6 mm, and 27.5 mm.

To prevent the breakup of caking fertilizer during the scanning process, the caking fertilizer was fixed. The three-dimensional model of caking fertilizer was obtained by scanning with an OKIO 5M 3-dimensional scanner, and the discrete metamodel of caking fertilizer was obtained by particle substitution. The radius of the small particles used for substitution was the equivalent diameter of the mother and daughter red composite fertilizer, and the contact model between the particles was set as the bonding contact model. The three-dimensional model of caking fertilizer is shown in Figure 3.

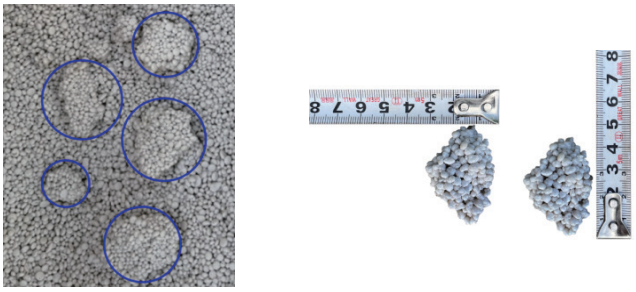

a. Fertilizer forms under natural conditions b. Long and short axes of caking fertilizers

Figure 2 Fertilizer considered for testing

a. Caking fertilizers b. Three-dimensional scanning of caking fertilizers c. Three-dimensional model of caking fertilizers

Figure 3 Three-dimensional scanning modeling of caking fertilizer

2.3 Uniaxial compression test of the caking fertilizer

2.3.1 Bench test of uniaxial compression

Randomly selected caking fertilizers were subjected to a compression crushing test by compressing them downward at 0.25 mm/s until the specimen appeared to stop crushing. The compression test is shown in Figure 4.

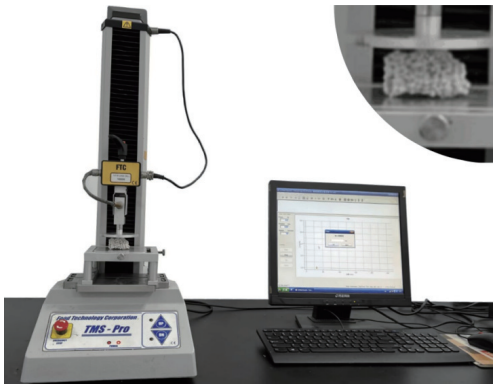

Figure 4 Uniaxial compression test of caking fertilizers

2.3.2 Simulation test of uniaxial compression

The test caking fertilizer was randomly sampled, and the uniaxial compression test simulation model was established through the caking fertilizer model and simulation parameter determination. The EDEM 2020 was used to establish the compression model, and the parameter settings were the same as those of the mass spectrometer test. The model is shown in Figure 5. The intrinsic parameters of the ABS material and the contact parameters between the material and fertilizer are described in the literature[7], and the simulation parameters of caking fertilizer are obtained via parameter calibration. The simulation parameters are listed in Table 1.

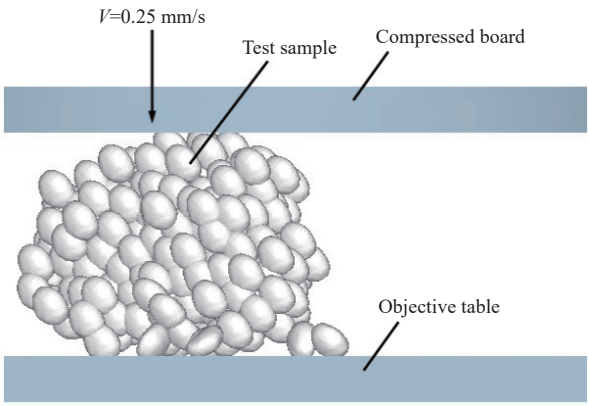

Figure 5 Uniaxial compression simulation test of caking fertilizer

The total EDEM simulation time was 6 s, and the data were saved every 0.001 s. To ensure that the caking model was initially

intact, the time step was set to 1.8×10^{-6} s, and the grid size was taken to be 2.5 times the smallest spherical cell body.

Table 1 Simulation parameters

Parameter	Value
Compound fertilizer Poisson's ratio	0.28
Compound fertilizer shear modulus/Pa	2.7×10^{8}
Compound fertilizer density/kg·m^{-3}	1122
ABS Poisson's ratio	0.394
ABS shear modulus/Pa	8.96×10^{8}
ABS density/kg·m^{-3}	1335
Restitution coefficient (interaction with compound fertilizer)	0.3
Static friction coefficient (interaction with compound fertilizer)	0.32
Rolling friction coefficient (interaction with compound fertilizer)	0.0881
Restitution coefficient (interaction with ABS)	0.34
Static friction coefficient (interaction with ABS)	0.45
Rolling friction coefficient (interaction with ABS)	0.03
Restitution coefficient (interaction with caking fertilizer)	0.10
Static friction coefficient (interaction with caking fertilizer)	0.53
Rolling friction coefficient (interaction with caking fertilizer)	0.12
Restitution coefficient (interaction between caking fertilizer and ABS)	0.25
Static friction coefficient (interaction between caking fertilizer and ABS)	0.49
Rolling friction coefficient (interaction between caking fertilizer and ABS)	0.08

2.4 Calibration method of the bonding model parameters for caking fertilizer

The bonding model parameters of the caking fertilizer were calibrated via simulation and physical tests, with the critical crushing force and critical crushing displacement as the response targets. A series of uniaxial compression tests was carried out using EDEM software, and the parameters of the bonding model for caking fertilizer were determined through tests such as the screening of crushing influencing factors, approximation of parameter ranges, and optimal parameter solving. The accuracy of the calibrated parameters was also verified through bench and field fertilizer discharge tests using the crushing rate as an indicator.

2.5 Validation of the parameters of the bonding model for caking fertilizer

To verify the accuracy of the calibrated parameters of the caking fertilizer bonding model, the designed four-head spiral two-row fertilizer discharger was used to carry out the validation of caking fertilizer crushing simulation with bench testing, and field discharge testing was also carried out to determine the caking fertilizer crushing rate. The simulation and bench validation tests are shown in Figure 6.

Figure 6 Simulation test for validation of the calibration parameters of the bonding model for caking fertilizer

The field validation test was carried out in the modern agricultural research base of Huazhong Agricultural University, as shown in Figure 7.

a. Bench test b. Field test

Figure 7 Bench and field testing of caking fertilizer for bonding model parameter calibration validation

In the test, the rotational speed of the fertilizer discharger was set at 30 r/min, and the speed of the conveyor belt and the forward speed of the tractor were controlled at 3.6 km/h. The quality of fertilizer in the nonparticulate state discharged from the fertilizer discharger was determined, and the average value was calculated by repeating the test for six groups. The equation for calculating the crushing rate of the caking fertilizer was

$$\varphi = \left(1 - \frac{m_2}{m_1}\right) \times 100\% \quad (1)$$

where, φ is the crushing rate of the caking fertilizer; m_1 is the total mass of caking fertilizer, g; m_2 is the mass of unbroken caking fertilizer, g.

3 Results and discussion

3.1 Calibration of bonding model parameters for caking fertilizer

3.1.1 Plackett-Burman test to screen for influencing factors

To examine the relationship between the response targets and the influencing factors, five parameters (x_1, x_2, x_3, x_4, and x_5), namely, the normal contact stiffness, tangential contact stiffness, critical normal stress, critical tangential stress, and bond radius, were taken as the influencing factors; the critical crushing displacement y_1 and critical crushing force y_2 were taken as the response targets; and the upper and lower values of the factors were taken to describe the range of the factor values to determine the significance of the factors. The ranges of the factors were determined by preliminary simulation. The Plackett-Burman test was used for analysis. The design of the test factor levels is listed in Table 2, and the results of the test are listed in Table 3[19,25-27].

Table 2 Plackett-Burman test factor code table

Code	Factor				
	x_1/N·m^{-3}	x_2/N·m^{-3}	x_3/Pa	x_4/Pa	x_5/mm
–1	3.0×108	4.0×107	2×104	1.5×104	1.75
1	6.0×108	7.0×107	3.5×104	3.0×104	2.00

Analysis of variance (ANOVA) and *t*-tests were performed on the factor-level influence effects using Design-Expert 11 software. The results of the analysis are shown in Table 4 and Figure 8.

The results of the analysis show that the factors x_2, x_4, and x_5 have significant effects on the critical crushing displacement y_1 and that the significance of the effect of each factor is in the order of x_5, x_2, x_4, x_3, and x_1. The factors x_3, x_4, and x_5 have significant effects on the critical crushing force y_2, and the significance of the effect of

each factor is in the order of x_5, x_3, x_4, x_1, and x_2. Through the t value test of the Pareto chart, it can be concluded that the factors with a significant effect on the response target have a positive effect on the response target.

The coding model of each factor with the critical crushing displacement and critical crushing force of caking fertilizer is as follows:

$$\begin{cases} y_1 = 5.67 + 0.0443x_1 + 0.5391x_2 - 0.1793x_3 + 0.3826x_4 + 1.13x_5 \\ y_2 = 10.25 + 0.445x_1 - 0.425x_2 + 1.21x_3 + 1.14x_4 + 2.38x_5 \end{cases} \tag{2}$$

3.1.2 Steepest ascent test to approximate the optimal parameters

Based on the results of factor screening, it can be seen that x_1 had no significant effect on the response target, so its median value of 4.5×10^8 N/m^3 was selected as the simulation parameter. The initial values of the significance factors x_2, x_3, x_4, and x_5 were set to be 4.0×10^7 N/m^3, 2.0×10^4 Pa, 1.5×10^4 Pa, and 1.75 mm, respectively, and the steepest ascent test was conducted with interval steps of 1.0×10^7 N/m^3, 0.5×10^4 Pa, 0.5×10^4 Pa, and 0.05 mm to further narrow the range of the optimal simulation parameters. The steepest ascent test factor scheme and results are listed in Table 5.

Table 3 Plackett–Burman test results

Serial number	x_1	x_2	x_3	x_4	x_5	y_1/mm	y_2/N
1	1	1	–1	1	1	8.32	11.445
2	–1	1	1	–1	1	6.34	11.445
3	1	–1	1	1	–1	4.32	11.605
4	–1	1	–1	1	1	7.89	13.005
5	–1	–1	1	–1	1	6.23	11.805
6	–1	–1	–1	1	–1	4.61	6.805
7	1	–1	–1	–1	1	5.98	12.585
8	1	1	–1	–1	–1	4.73	4.585
9	1	1	1	–1	–1	4.88	8.485
10	–1	1	1	1	–1	5.12	9.985
11	1	–1	1	1	1	6.08	15.465
12	–1	–1	–1	–1	–1	3.59	5.785

Table 4 Analysis of the significance of parameters

Source of variation	y_1					y_2				
	Sum of squares	Degrees of freedom	Mean square	F	p	Sum of squares	Degrees of freedom	Mean square	F	p
Model	21.04	5	4.21	24.81	0.0006*	105.4	5	21.08	14.01	0.0029*
x_1	0.0235	1	0.0235	0.1386	0.7225	2.38	1	2.38	1.58	0.2555
x_2	3.49	1	3.49	20.56	0.004*	2.17	1	2.17	1.44	0.2752
x_3	0.3856	1	0.3856	2.27	0.1823	17.71	1	17.71	11.78	0.0139*
x_4	1.76	1	1.76	10.36	0.0182*	15.46	1	15.46	10.28	0.0185*
x_5	15.39	1	15.39	90.74	<0.0001*	67.69	1	67.69	45	0.0005*
Residual	1.02	6	0.1696			9.03	6	1.5		
Sum	22.06	11				114.43	11			

Note: * indicates a significant difference (p<0.05) in this and the following tables.

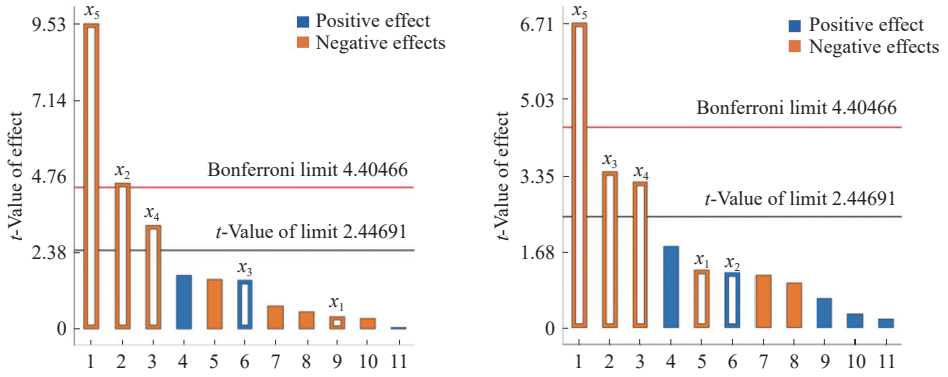

a. The order of significance of critical breaking displacement b. The order of significance of critical breaking force

Figure 8 Pareto chart

Table 5 Scheme and results of the steepest ascent test

Serial number	x_1/N·m^{-3}	x_2/N·m^{-3}	x_3/Pa	x_4/Pa	x_5/mm	y_1/mm	y_2/N
1	4.5×10^8	4.0×10^7	2.0×10^4	1.5×10^4	1.75	4.539	5.167
2	4.5×10^8	5.0×10^7	2.5×10^4	2.0×10^4	1.80	4.719	9.849
3	4.5×10^8	6.0×10^7	3.0×10^4	2.5×10^4	1.85	5.513	11.236
4	4.5×10^8	7.0×10^7	3.5×10^4	3.0×10^4	1.90	6.866	14.048
5	4.5×10^8	8.0×10^7	4.0×10^4	3.5×10^4	1.95	7.236	16.614
6	4.5×10^8	9.0×10^7	4.5×10^4	4.0×10^4	2.00	8.413	19.544

The critical crushing displacement and critical crushing displacement load in the caking fertilizer compression test were 5.75 mm and 11.946 N, respectively. The test results listed in Table 5 indicate that the error between the response target and the spectrometer test values in the simulation first decreases and then increases, in which the critical crushing displacement and critical crushing force of the simulation values in group 3 are closest to those of the spectrometer test values.

3.1.3 Box–Behnken test to determine optimal parameters

To improve the accuracy of the simulation results, based on the results of the steepest ascent test, and according to the principle of Box–Behnken design, the significance factors in group 2 and group 4 were selected as the high and low levels of the Box–Behnken test, respectively, and the values of the insignificance factors were consistent with those of the steepest ascent test. The levels of the test factors are listed in Table 6; the test program and results are listed in Table 7.

Table 6 Box–Behnken test factor level table

Code	Factor				
	x_1/N·m^{-3}	x_2/N·m^{-3}	x_3/Pa	x_4/Pa	x_5/mm
–1	4.5×10^8	5.0×10^7	2.5×10^4	2.0×10^4	1.80
0	4.5×10^8	6.0×10^7	3.0×10^4	2.5×10^4	1.85
1	4.5×10^8	7.0×10^7	3.5×10^4	3.0×10^4	1.90

The second-order regression equations modeling the response targets y_1 and y_2 with the four factors were modeled using the Design-Expert R11.0, respectively:

$$y_1 = 5.741 + 0.0643x_1 + 0.273x^2 + 0.342x_3 + 0.542x_4 - 0.007x_1x_2 + 0.0403x_1x_3 + 0.0208x_1x_4 + 0.028x_2x_3 + 0.0195x_2x_4 - 0.111x_3x_4 - 0.0287x_1^2 - 0.112x_2^2 - 0.112x_3^2 + 0.145x_4^2 \quad (3)$$

$$y_2 = 11.916 - 0.0242x_1 + 0.426x_2 + 0.636x_3 + 1.131x_4 + 0.047x_1x_2 - 0.0303x_1x_3 + 0.157x_1x_4 + 0.0965x_2x_3 + 0.108x_2x_4 - 0.0248x_3x_4 - 0.157x_1^2 - 0.112x_2^2 - 0.029x_3^2 + 0.145x_4^2 \quad (4)$$

Table 8 shows the ANOVA results of the quadratic polynomial regression model. The results show that the model p is less than 0.0001, which indicates that the model results are significant, and the mismatch term is not significant, which indicates that the model is highly credible. x_3, x_4, and x_5 have a significant effect on the response target, and the significance of the effect is in the order of x_5, x_4, and x_3. Narrowing down the range of the constraints helps to determine the optimal combinations of the simulation parameters.

Table 7 Box–Behnken test scheme and results

Serial number	x_2/N·m^{-3}	x_3/Pa	x_4/Pa	x_5/mm	y_1/mm	y_2/N
1	–1	–1	0	0	5.394	11.147
2	1	–1	0	0	5.423	11.196
3	–1	1	0	0	5.790	11.819
4	1	1	0	0	5.791	12.056
5	0	0	–1	–1	4.930	10.163
6	0	0	1	–1	5.779	11.448
7	0	0	–1	1	5.990	12.481
8	0	0	1	1	6.395	13.666
9	–1	0	0	–1	5.239	11.018
10	1	0	0	–1	5.373	10.574
11	–1	0	0	1	6.401	12.931
12	1	0	0	1	6.618	13.115
13	0	–1	–1	0	4.940	11.011
14	0	1	–1	0	5.566	11.483
15	0	–1	1	0	5.513	11.884
16	0	1	1	0	6.251	12.742
17	–1	0	–1	0	5.095	11.108
18	1	0	–1	0	5.210	11.010
19	–1	0	1	0	5.813	12.683
20	1	0	1	0	6.089	12.464
21	0	–1	0	–1	4.852	10.434
22	0	1	0	–1	5.388	11.343
23	0	–1	0	1	6.025	12.512
24	0	1	0	1	6.639	13.853
25	0	0	0	0	5.852	11.798
26	0	0	0	0	5.612	11.792
27	0	0	0	0	5.711	11.733
28	0	0	0	0	5.658	12.021
29	0	0	0	0	5.872	12.236

Table 8 ANOVA of the Box–Behnken test

	y_1					y_2				
	Sum of squares	Degrees of freedom	Mean square	F	p	Sum of squares	Degrees of freedom	Mean square	F	p
Source of variation										
Model	6.31	14	0.4504	23.42	<0.0001*	23.05	14	1.65	39.61	<0.0001*
x_2	0.0498	1	0.0498	2.59	0.1297	0.0071	1	0.0071	0.1716	0.6849
x_3	0.8957	1	0.8957	46.58	<0.0001*	2.18	1	2.18	52.38	<0.0001*
x_4	1.41	1	1.41	73.12	<0.0001*	4.86	1	4.86	116.81	<0.0001*
x_5	3.53	1	3.53	183.44	<0.0001*	15.36	1	15.36	369.59	<0.0001*
x_2x_3	0.0002	1	0.0002	0.0097	0.9228	0.0088	1	0.0088	0.2124	0.652
x_2x_4	0.0065	1	0.0065	0.3363	0.5712	0.0037	1	0.0037	0.0885	0.7705
x_2x_5	0.0017	1	0.0017	0.0876	0.7716	0.0985	1	0.0985	2.37	0.146
x_3x_4	0.0032	1	0.0032	0.1647	0.691	0.0373	1	0.0373	0.8976	0.3595
x_3x_5	0.0015	1	0.0015	0.0796	0.7819	0.0467	1	0.0467	1.12	0.3072
x_4x_5	0.0491	1	0.0491	2.55	0.1323	0.0025	1	0.0025	0.0593	0.8112
x_{22}	0.0054	1	0.0054	0.2792	0.6055	0.1599	1	0.1599	3.85	0.0701
x_{32}	0.081	1	0.081	4.21	0.0593	0.0816	1	0.0816	1.96	0.1831
x_{42}	0.081	1	0.081	4.21	0.0593	0.0056	1	0.0056	0.134	0.7198
x_{52}	0.1368	1	0.1368	7.11	0.0184*	0.1366	1	0.1366	3.29	0.0914*
Residual	0.2692	14	0.0192			0.5819	14	0.0416		
Aberrant term	0.2154	10	0.0215	1.6	0.3445	0.4057	10	0.0406	0.9205	0.5861
Sum	6.57	28				23.63	28			

According to the physical test target values y_1=5.75 mm and y_2=11.946 N, Table 7 shows that the simulated response target values of test combinations 3, 4, and 27 are closest to the physical test values. The ANOVA results reveal that factor x_5 was the most significant factor influencing the response target, x_4 had the second most significant impact on the response target, x_3 had a relatively

small impact on the response target, and x_2 did not have a significant impact on the response target. Therefore, the optimal simulation parameter combination constraint range was set as

$$\begin{cases} y_1 = 5.750 \\ y_2 = 11.946 \\ 1.80 \le x_5 \le 1.90 \\ 2.0\times10^4 \le x_4 \le 3\times10^4 \\ x_3 = 3.0\times10^4 \\ x_2 = 6.0\times10^7 \end{cases} \tag{5}$$

The optimal combination of the x_3, x_4, and x_5 parameters was determined to be 3.0×10^4 Pa, 2.7568×10^4 Pa, and 1.8305 mm, respectively, by optimally solving the simulation parameters for the reduced range using Design Expert 11.

3.2 Simulation and comparison of uniaxial compression tests of caking fertilizer

To comply with the actual distribution principle of caking fertilizer, the test was conducted with a random sampling of caking fertilizer, and the test was repeated six times to obtain the average value. The displacement of the caking fertilizer during crushing was 5.750 mm, and the crushing force was 11.946 N. The optimized simulation parameters were used to simulate the compression crushing of the caking fertilizer. The critical crushing displacement and the critical crushing force were 5.767 mm and 11.987 N, respectively, and the relative errors between the simulation and the physical test values were 0.296% and 0.343%, respectively.

Figure 9 shows the simulated and actual force–displacement curves of caking fertilizer crushing, and the force changes in the caking fertilizer can be divided into three stages. At the initial stage of the test, the caking fertilizer is compressed and plastically deformed, and some particles are separated from the whole. At the middle stage, the core bonding area of the caking fertilizer is broken, and the force peaks, which is the point of breaking of the caking fertilizer. At the later stage, as the compression continues to decrease, the force continues to decrease, and the caking fertilizer becomes broken. Through comparative analysis, it can be seen that the force–displacement curve obtained from the simulation is consistent with the actual curve. Figure 10 shows the comparison between the physical test and simulation of various stages of caking fertilizer loading and crushing, and the light blue in Figure 10b shows the bonds. The crushing states of the caking fertilizer at each stage of the physical test and simulation are consistent, indicating that the calibrated discrete element simulation bonding parameters of the caking fertilizer are sufficiently accurate and can be used in the simulation of the caking fertilizer crushing process.

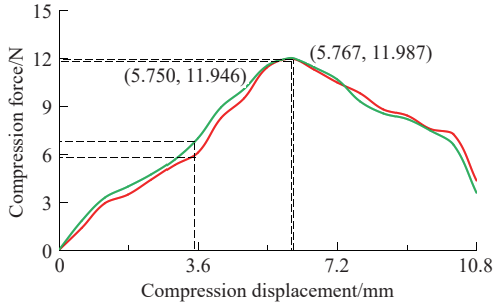

Figure 9 Simulated and actual displacement–force curves

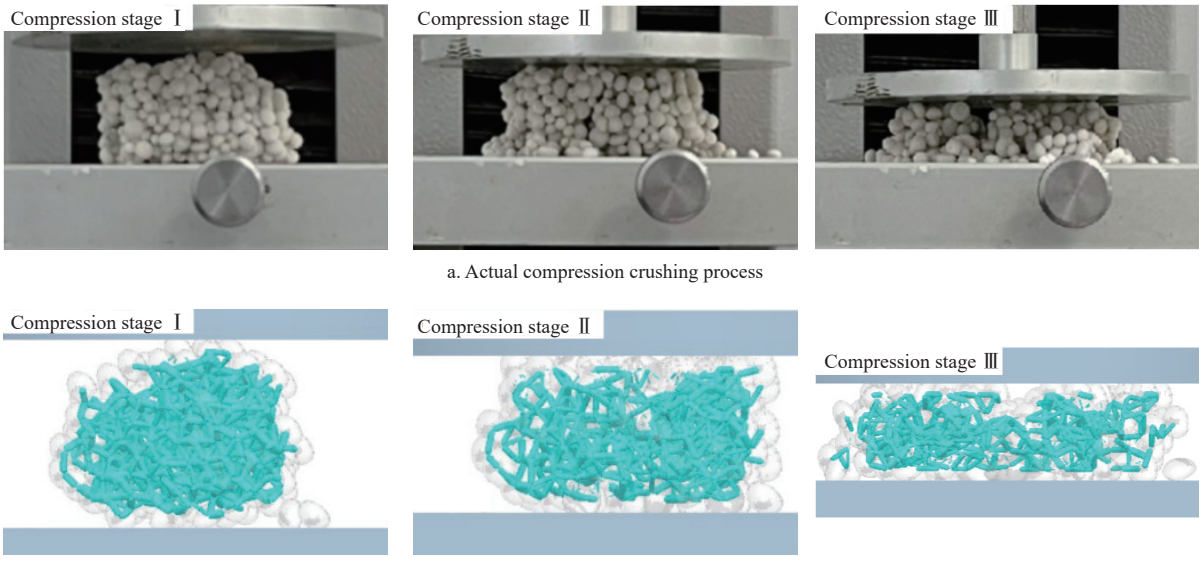

a. Actual compression crushing process

b. Simulated compression crushing process

Figure 10 Simulated and actual caking fertilizer crushing process

3.3 Verification test of the caking fertilizer crushing rate

Figure 11 shows the different positional morphologies during the simulated test of caking fertilizer crushing, without showing the granular compound fertilizer. The caking fertilizer collides and squeezes with the knot-breaking device and the shell of the fertilizer discharger and the fertilizer discharging screw and rubs against the group of fertilizer particles, which leads to the breakage of the bonds between fertilizer particles (the light blue short lines between fertilizer particles are the bonds).

As seen from the simulation process, the caking fertilizer is broken into fertilizer lumps of different sizes under the collision and extrusion of the cracking device and the shell of the fertilizer discharger, and then it is further broken under the joint action of the fertilizer particle flow, the bonding breaking device, and the fertilizer discharging helix, turning into small fertilizer clusters and granular fertilizer discharging out of the fertilizer discharger.

Figures 12a and 12b show the simulation and bench test effects, and Figure 12c shows the field test effects. In Figure 12a, the black color indicates the discharged fertilizer, and some is in the form of small clumps. The circled fertilizer in Figure 12b is in the form of small clumps. This shows that some unbroken fertilizer clumps remain in both the simulation and actual discharged fertilizer tests.

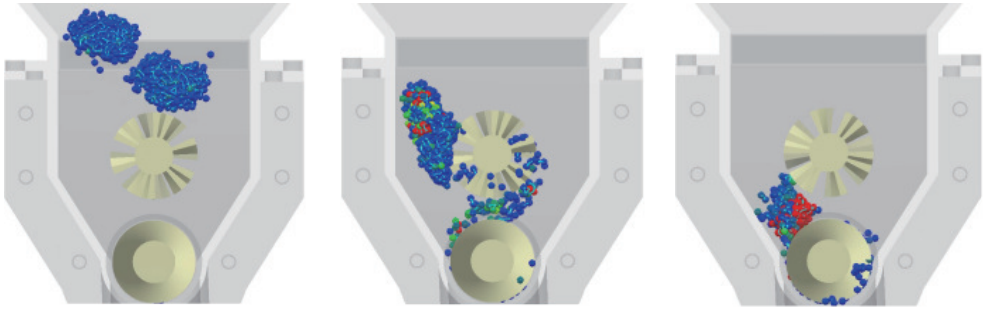

a. Located above the knot breaker b. Located in the center of the knot breaker c. Located between the knot breaker and the fertilizer screw

Figure 11 Forms of caking fertilizers in different locations

a. Simulated test b. Bench test c. Field test

Figure 12 Effect diagram of the test

The results of the simulation, bench test, and field test of caking fertilizer crushing showed that the crushing rate of the simulation was 88.78%, the crushing rate of the bench test was 83.62%, and the crushing rate of the field test was 93.28%. The relative errors between the simulation and bench and field tests were 5.81% and 5.06%, respectively, indicating that the accuracy of the combined parameters of the calibrated bonding model is high, which can provide a reference value for the simulation study of caking fertilizer.

4 Conclusions

In this work, compression crushing testing for a seeding and fertilizing apparatus indicated that the critical crushing displacement of caking fertilizer was 5.750 mm and that the critical crushing force was 11.946 N. A three-dimensional model of caking fertilizer was obtained by scanning, and a discrete element model of caking fertilizer was obtained via the bonding contact model. The results of the Plackett-Burman tests showed that the tangential contact stiffness, the critical tangential stress, and the bond radius have a significant influence on the critical crushing displacement. The results of the Box-Behnken tests showed that the critical normal stress, critical tangential stress, and bond radius have a significant influence on the critical crushing displacement and critical crushing force. The critical crushing displacement and critical crushing force under the optimal parameter combination were 5.767 mm and 11.987 N, respectively, and the relative errors with the test values of the mass spectrometer were 0.296% and 0.343%, respectively. The results of the validation test on the crushing of caking fertilizers carried out by the four-head spiral two-row fertilizer discharger showed that at a speed of 30 r/min of the discharger, the crushing rate was 88.78% in the simulation test, and the crushing rates were 83.62% and 93.28% in the bench test and field test, respectively. The relative errors between the crushing rate of the simulation and those of the bench test and the field test were 5.81% and 5.06%, respectively, which supports the validation results of the simulated test and thus the reliability of the combined parameters of the calibrated bonding model.

Acknowledgements

This research was financially supported by the China Agricultural Research System of MOF and MARA (NO: CARS-12).

[References]

[1] Wan X Y, Liao Q X, Liao Y T, Ding Y C, Zhang Q S, Huang H, Zhu L T. Situation and prospect of key technology and equipment in mechanization and intelligentization of rapeseed whole industry chain. Journal of Huazhong Agricultural University, 2021; 40(2): 24–44. (in Chinese).

[2] Chen H, Gao L P, Chen Y, Lin J X, Liao Y T, Liao Q X. Effects of mechanical direct seeding synchronous deep fertilization on winter rapeseed stem lodging resistance and yield. Transactions of the CSAE, 2022; 38(5): 20–27. (in Chinese).

[3] Lu J W, Ren T, Li X K, Cong R H, Lu Z F, Zhang Y Y, Zhu J. Strategy of precisely controlling nutrient and system of efficient fertilization technology for winter rapeseed in China. Journal of Huazhong Agricultural University, 2023; 42(6): 18–25. (in Chinese).

[4] Xiao W L, Xiao W F, Liao Y T, Zhang Q S, Wei G L, Liao Q X. Design and performance test of plough-type positive deep fertilization device for rapeseed direct planter. Journal of Huazhong Agricultural University, 2018; 37(4): 131–137. (in Chinese).

[5] Xiao W L, Liao Y T, Shan Y Y, Li M L, Wang L, Liao Q X. Design and experiment of quad-screw double-row fertilizer apparatus for rape seeding machine. Transactions of the CSAM, 2021; 52(11): 68–77. (in Chinese).

[6] Zhang W. Study on moisture absorption and caking and their prevention of compound fertilizer. MS desertation, East China University of Science and Technology, 2012.

[7] Xiao W L, Chen H, Wan X Y, Li M L, Liao Q X. Influence of shape and particle size distribution on discrete element simulation flow characteristics of granular compound fertilizers. Applied Engineering in Agriculture, 2021; 37(6): 1169–1179.

[8] Song X F, Zhang W F, Dai F, Zhao W Y, Yang J, Zhang X K. Parameter optimization for fertilizer block crushing device of fertilizer machine based on discrete element method. Journal of HuHan Agricultural University (Natural Sciences), 2017; 43(2): 206–211. (in Chinese).

[9] Liu C L, Wei D, Song J N, Li Y N, Du X, Zhang F Y. Systematic study on boundary parameters of discrete element simulation of granular fertilizer. Transactions of the CSAM, 2018; 49(9): 82–89. (in Chinese).

[10] Niu Z Y, Kong X R, Shen P S, Li H C, Geng J, Liu J. Parameters calibration of discrete element simulation for pellet feed attrition. Transactions of the CSAM, 2022; 53(7): 132–140, 207. (in Chinese).

[11] Potyondy D O, Cundailp A. A bonded-particle model for rock. Interrnational Journal of Rock Mechanics and Mining Sciences, 2004; 41(8): 1329–1364.

[12] Cleary P W, Sinnott M D. Simulation of particle flows and breakage in crushers using DEM: Part 1-Compression crushers. Minerals Engineering, 2015; 74: 178–197.

[13] Zhang J X, Zhang P, Zhang H, Tan C L, Wan W Y, Wan Y C. Discrete element simulation parameters calibration for Xinjiang cotton straw. Transactions of the CSAM, 2024; 55(1): 76–84, 108. (in Chinese).

[14] Bussmann S, Kruggel-Emden H, Reichert M. Realizing fragment spawning and fragment growth in the parallelized discrete element method (DEM) during modelling of comminution. Advanced Powder Technology, 2021; 32(7): 2171–2191.

[15] Jia H L, Deng J Y, Deng Y L, Chen T Y, Wang G, Sun Z J. Contact parameter analysis and calibration in discrete element simulation of rice straw. Int J Agric & Biol Eng, 2021; 14(4): 72–81.

[16] Wang H B, Pan Z P, WU L T Y, Wang C G, Ma Z. Parameter calibration of discrete element model for simulation of crushed corn stalk screw conveying. Journal of Agricultural Science and Technology, 2023; 25(3): 96–106. (in Chinese).

[17] M, Z T, Zhao Z H, Quan W, Shi F G, Gao C, Wu M L. Calibration of discrete element parameter of rice stubble straw based on EDEM. Journal of Agricultural Science and Technology, 2023; 25(11): 103–113. (in Chinese).

[18] Liao Y, Wang Z, Liao Q, Liang F, Liu J. Calibration of discrete element parameters of fodder rape crop stem at flowering stage. 2020 ASABE Annual International Meeting. 2020; 20201513: 1–9. DOI: 10.13031/aim.202001513.

[19] Liao Y T, Liao Q X, Zhou Y, Wang Z T, Jiang Y J, Liang F. Parameters Calibration of discrete element model of fodder rape crop harvest in bolting stage. Transactions of the CSAM, 2020; 51(6): 73–82. (in Chinese).

[20] Zhang Z G, Zeng C, Xing Z Y, Xu P, Guo Q F, Shi R M, et al. Discrete element modeling and parameter calibration of safflower biomechanical properties. Int J Agric & Biol Eng, 2024; 17(2): 37–46.

[21] Zhang F W, Song X F, Zhang X K, Zhang F Y, Wei W C, Dai F. Simulation and experiment on mechanical characteristics of kneading and crushing process of corn straw. Transactions of the CSAE, 2019; 35(9): 58–65. (in Chinese).

[22] Zhang X R, Hu X H, Liu X J, Yang Y M, Li A. Calibration and verification of bonding parameters of banana straw simulation model based on discrete element method. Transactions of the CSAM, 2023; 54(5): 121–130. (in Chinese).

[23] Chen ., Wang Q, Xu D, Li H, He J, Lu C. Design and experimental research on the counter roll differential speed solid organic fertilizer crusher based on DEM. Computers and Electronics in Agriculture, 2023; 207: 107748. DOI: 10.1016/j.compag.2023.107748.

[24] Chen G, Wang Q, Li H, He J, Lu C, Xu D, Sun M. Experimental research on a propeller blade fertilizer transport device based on a discrete element fertilizer block model. Computers and Electronics in Agriculture, 2023; 208: 107781.

[25] Yuan Q C, Xu L M, Xing J J, Duan Z Z, Ma S, Yu C C, Chen C. Parameter calibration of discrete element model of organic fertilizer particles for mechanical fertilization. Trans. CSAE, 2018; 34(18): 21–27. (in Chinese)

[26] Chen G B, Wang Q J, Li W Y, He J, Li H W, Yu C C. Design and experiment of double roller differential speed crushing fertilizer device for block organic fertilizer. Transactions of the CSAM, 2021; 52(12): 65–76. (in Chinese)

[27] Du X, Liu C L, Jiang M, Yuan H, Dai L, Li F L. Calibration of bonding model parameters for coated fertilizers based on discrete element method. Transactions of the CSAM, 2022; 53(7): 141–149. (in Chinese)